AN OVERVIEW OF THE NUMERICAL MODELLING AND MONTE CARLO SIMULATION OF REHEATING FURNACES

Abstract

Extensive research has been conducted in the past 30 years to investigate the heat characteristics of sheet/sheets in different furnaces featuring an emerging thermal environment. The study comprises two approaches: numerical modelling using CFD and the Monte Carlo method. Numerical modelling using commercial codes for industrial scales has been documented. This methodology involves solving the Navier-Stokes equations, which are based on conservation equations for mass, momentum, energy, and species. The goal is to predict the heat transfer from radiation into the reheating furnace enclosure and the conductive heat transfer within the steel slabs. Monte Carlo simulation was employed to derive the view factor matrix in a separate investigation. Various methods were employed to solve conduction and radiation problems and predict plate temperature profiles. Different categories of research encompass a wide range of modelling techniques and methodologies. These include the study of turbulent jet flow of fuel gases, convective and radiative phenomena in furnaces, slab conduction phenomena, and the calculation of view factor matrix.

Keywords: Reheating furnaces, CFD, Steelmaking, Monte Carlo Simulation.

Authors

Abhinav Maurya
Department of Metallurgical
and Materials Engineering
Indian Institute of Technology Ropar
Punjab, India.

Prvan Kumar Katiyar
Department of Metallurgical
and Materials Engineering
National Institute of Technology Srinagar
Jammu and Kashmir, India.

Prince Kumar Singh
Department of Metallurgical
and Materials Engineering
Indian Institute of Technology Ropar
Punjab, India.
princeks@iitrpr.ac.in

I. INTRODUCTION

The reheating furnaces utilised in steel mills are responsible for the thermal treatment of plates, ingots, billets, and blanks, with the primary objective of attaining consistent and ideal rolling temperatures. Heating furnaces can be categorised into two types: intermittent (batch) or continuous. Continuous forms of furnaces encompass several designs, such as pusher furnaces, rotary furnaces, moving beams, and roller hearths. Aviary heaters are often regarded as advanced and cutting-edge in all of these scenarios. The furnaces are fuelled by a direct supply of gas, mostly consisting of natural gas, coke gas, blast furnace exhaust, or other combinations thereof. Moving beam heating furnaces are commonly employed in the process of heating steel plates or billets with diverse sizes and dimensions. The grater/batter has the capability to be charged at various temperatures, including ambient temperature sourced from the tank, warm temperature directly from the continuous charger, and room temperature.

Reheating procedure frequently includes the use of distinct sheet grades, while maintaining a consistent sheet size. As the board or battery traverses various temperature zones, its temperature escalates in accordance with the temperature of each respective furnace zone. Nevertheless, the temperature rates in the preheat and reheat zones exhibit an increase as a result of the firing rates seen in the distinct furnace zones. The experimental setup involves subjecting the low temperature plate, typically maintained at 27 °C, to a high temperature furnace operating within the range of 1260-1280°C. The implementation of a low heating rate effectively mitigates the formation of thermal strains. Subsequently, the plate is subjected to intense heating within an annealing zone, whereby the temperature necessary for absorption is carefully sustained. This process ensures the attainment of a consistent temperature throughout the plate, facilitating subsequent rolling procedures. The homogeneity of grain size throughout the entirety of the steel slabs/billets is influenced by the heating quality and the efficiency of the reheating process, potentially influencing the mechanical properties of the final products. The heating efficiency of slabs in industrial reheating operations is influenced by several aspects related to the combustion process, including as the design of the burner, the ratio of air to gas, the construction of furnace, and the materials used for refractory purposes.

This study is divided into two sections. The first part focuses on numerical modelling, employing widely-used commercial computational fluid dynamics (CFD) software such as FLUENT, STAR-CD, and PHOENICS. These softwares utilise the finite volume method (FVM) to solve equations regulating the flow of hot gases and combustion in the reheat furnace, including the Navier-Stokes equations and energy conservation equations. The subsequent phase of the investigation relies on the utilisation of the Monte Carlo method to simulate and acquire the view factor matrix, with the objective of optimising heat transfer. The primary factor in the calculation of thermal radiation is the heat exchange between surfaces within a furnace enclosure, which is given by the view-factor matrix.

1. **Reheating Furnaces in Steel Industries:** The primary objective of reheating activities is to attain uniform temperatures in slabs and billets, hence enhancing their malleability for subsequent rolling processes. The optimisation of the fuel feeding rate and the air-to-fuel mixture in the burners located in different zones of the reheating furnace is employed to attain the desired rolling temperature. The heating efficiency of the reheating furnace is

determined by the duration of hot flue gas interaction with the stock and the length of flames. The length of the flame is determined by the rate of fuel/air flow. The thermo-physical properties of materials, including thermal conductivity and specific heat, play a significant role in determining the rate at which steel slabs and billets undergo heating.

When exposed to flames, hot furnace walls and radiation emitted by hot combustion gases, the surface temperature of a steel slab experiences a substantial increase. Radiation serves as the predominant mechanism for heat transmission within a reheating furnace. The reheating furnace is often divided into three to five temperature zones based on its length, with the temperature increasing in the longitudinal direction of the furnace. The temperature of steel slabs is elevated within the reheating furnace to attain the requisite range that imparts the desired plastic properties essential for the subsequent rolling process. The utilisation of reheating furnaces is an essential aspect within the operations of rolling mills. The principal objective of subjecting materials to heating is to induce softening for subsequent rolling operations by establishing an initial temperature that is adequately elevated, such that rolling occurs within a temperature range that is entirely austenitic[1][2][3][4].

Continuous type reheat furnaces can be classified into five distinct categories: rotary hearth, walking hearth, pusher type, continuous re-circulating bogie and walking beam furnace type. The pusher type and walking beam type are commonly employed reheating furnaces for the purpose of heating billets, ingots, and slabs that possess diverse initial thermal conditions. The typical walking beam type reheating furnace (WB furnace) exhibits consistent and uniform heating of slabs, blooms and billets to achieve the required temperature, while simultaneously limiting the occurrence of skid marks[4].The design factors and operational conditions have a crucial role in determining various aspects of the rolled product, including its quality, production rate, energy consumption, environmental impact in terms of pollutants, and economic viability.
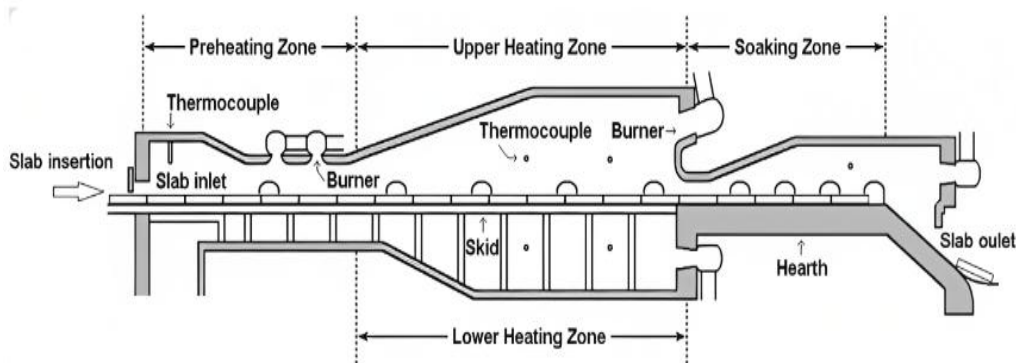

Figure 1: Schematic of Pusher Type Reheating Furnace[5]

The walking beam type furnace (WB furnace) can be categorised into either three zones or five zones. The three zones include preheating, heating and soaking. Alternatively, the five zones consist of non-firing, charging, preheating, heating and soaking. The steel slabs that are introduced into the non-firing zone are conveyed to the subsequent zone using a walking beam mechanism, operating at a predetermined velocity.

The length of the furnace ranges from 35 to 40 metres, while its height in each zone is determined by slopes that connect the upper portion to its dam-shaped lower section. The quantity of slabs and burners is contingent upon the dimensions of the reheating furnace. Reheating furnaces are commonly characterised by their dimensions, which normally measure 9 metres in length, 1.16 metres in width, and 0.23 metres in height. These furnaces are designed to accommodate a simultaneous heating of 28 to 30 slabs, with a uniform spacing of 0.2 metres between each slab. The slab remains in the reheating furnace for a duration of 180-200 minutes. The reheating furnace was equipped with a total of 50 burners, consisting of 24 axial burners located in the upper zone and 26 side burners situated in the bottom zone.
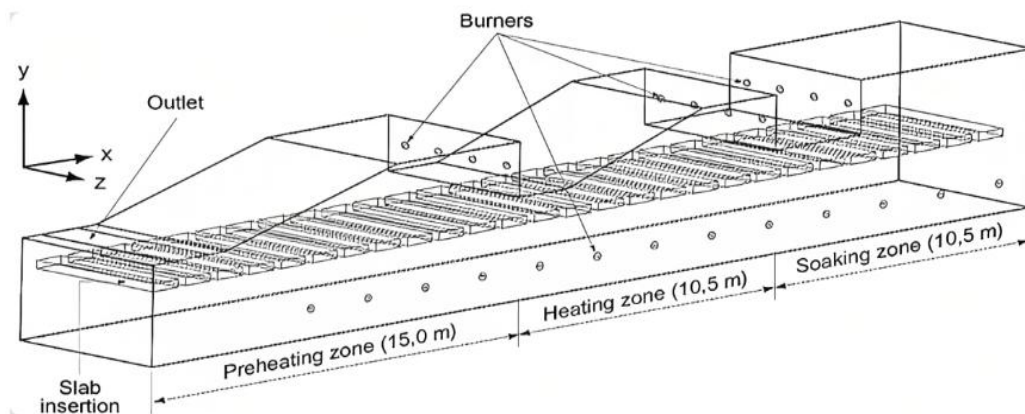

Figure 2: Schematic of Walking Beam Type Reheating Furnace(WB furnace) without Skid Beam Arrangement[6]

2. **Heat Transfer Mechanisms in Reheating Furnace:** Reheating transfer involves all three heat transfer mechanisms:

- Conduction between a solid charge material and the furnace wall;
- Convection between hot combustion gases; and
- Radiation heat transfer between walls, flame, combustion gases, and hot slabs present in the furnace.

In a reheat furnace, the radiation mechanism of heat transfer predominates. Radiation heat transfer is used to warm 92% of the steel stocks to a particular temperature. The development of skid marks is caused by the skid assembly inside the furnace enclosure, which prevents radiation from reaching the slabs. Heat is transferred to the steel slabs or billets during heating, raising the temperature over the recrystallization temperature (1250°C). Depending on the conditions, the charging temperature of steel slabs or bills might range from 28°C to 800°C. The temperature gradient and surface temperature of the steel slabs serve as indicators of steel quality. The number of zones that can vary in reheat furnace depends on the design and size of the furnace, skid design, refractory used, and fuel preheating. All these factors have significant impact on the reheating furnace's energy efficiency [3][7].

3. **Impact of Flame Characteristics on Heat Transfer:** The predominant mode of heat transfer during the heating process of steel slabs or a charge in a reheating furnace is widely recognised to be radiation. The flame of the reheat furnace, characterised by its highest temperature, emits thermal energy to both the furnace wall and the steel surface. Consequently, the heat transfer is significantly influenced by the shape, length, and characteristics of the flame. The composition of fuel (combining coal gasification and blast furnace gas), the design of the burner, and different rates of fuel and air flow can all have an impact on it. Effective mixing leads to the generation of a flame of superior quality. Consequently, the presence of high turbulence velocity induces the formation of short, bushy flames, thereby enhancing the convective heat transfer rate within the furnace enclosure. Insufficient or delayed complete mixing of the fuel and oxidizer might result in the formation of an elongated and slender flame. The utilisation of suitable adiabatic flame temperature leads to increased throughput and enhanced efficiency of the reheating furnace[1].

4. **Energy Optimization in Reheating Furnaces:** The dimensions and configuration of the reheat furnace play a critical role in the process of slab reheating, sometimes referred to as charge or load reheating. The design should be formulated with the objective of optimising the amount of charge that can be uniformly heated to a temperature acceptable for continued operation within a specified timeframe, while minimising the use of fuel and effort. The task can be accomplished by encapsulating the specified criteria [3][4][8]:

- Calculating the amount of heat to be applied to the charge.
- The production of sufficient heat inside the furnace to warm the charge and offset any potential losses.
- The transport of heat from furnace enclosure to charge surface.
- Steel stock's stock temperature consistency.
- Lowering the reheat furnace's heat losses.

In order to mitigate pollution, decrease the overall energy consumption per metric tonne of steel heated in reheating furnaces, and enhance global competitiveness in the steel products market, it is imperative to enhance equipment design and optimise operational parameters for steel rolling. Achieving a higher degree of temperature homogeneity throughout the rolling process can lead to improved thermomechanical characteristics of steel. The maintenance of a consistent temperature for the steel stock at the end of the heating process is crucial for reducing energy expenses and preventing the occurrence of metal flaws. In order to expedite industrialization and promote ecological sustainability in the present, it is imperative to embrace current heating trends, criteria, control systems, and technology. In order to enhance energy efficiency, the procedures of the walking beam type furnace are automated[3][4][7].

5. **Improper Heating of Stock in Reheating Furnace:** The heating rates of the steel stock vary across different regions within the reheat furnace enclosure. In order to mitigate the risks of overheating, burning, or melting of the steel stock, as well as to minimise the occurrence of thermal strains, it is imperative to effectively control the rate at which the steel stock absorbs heat. During the initial stage of the heating process, the rate of heating is comparatively high and then decreases in the subsequent zone. Failure to manage this

transition appropriately may result in an uneven dispersion of thermal energy within the material being heated. The challenges pertaining to stock heating might be attributed to the inherent limitations in the design capabilities and suboptimal operational performance of the reheat furnaces[4][9].

6. Primary Factors Affecting Fuel Consumption in Reheat Furnace:

- To ensure a smooth operation, the rolling capacity and reheat furnace capacity must match as extended residence time increases fuel consumption.
- Due to cold air infiltration, too much air being used, heat losses furnace walls and radiation losses from the furnace opening, a significant percentage of heat is lost from the furnace.
- The automation of the furnace's pressure and temperature control system reduces the fuel consumption.
- Fuel consumption is decreased by using the right combustion equipment and having the right fuel/air ratio.
- Improper maintenance and ineffective recuperators might increase fuel usage.

Several mathematical models and methodologies have been developed and successfully implemented in various furnace geometries to predict the heating behaviour of steel slabs or billets in a reheating furnace. The present investigations can be categorised into two distinct groups for the purpose of facilitating comprehension. The initial methodology involves solving the Navier-Stokes equations and energy conservation equations to govern the combustion process and the flow of hot gases within a furnace. The initial approach is characterised by its simplicity and cost-effectiveness in comparison to the alternative method. Furthermore, it encompasses the same comprehensive information as the latter approach, albeit with the prerequisite of experimental data. However, computational fluid dynamics (CFD) simulations are utilised to predict the thermal and reactive fluid characteristics of a furnace used for heating slabs. The second approach utilises real-time simulation or mathematical models, namely those based on the Monte Carlo method. These models are employed to determine the view factor matrix and analyse the thermal behaviour of the slabs within reheating furnaces. Additionally, they are utilised to solve the radiation transfer occurring within the furnace.

II. NUMERICAL MODELLING

1. **Previous Studies:** In a WB furnace, the modelling of radiation-dominant processes occurring within reheating furnaces is a necessary requirement. A radiative heat transfer model is employed in order to ascertain the radiation flux on the surface of a slab. Radiation is the mode of heat transfer observed in the context of hot combustible gases, walls, flames, and slabs. The use of Newton's law of cooling is employed to model the convection-induced heat transfer occurring between combustible flue gases, slabs, and furnace walls. The transient heat conductive model is employed to simulate the conductive heat transfer occurring in steel slabs and furnace walls. The temperature, composition of combustible gas, and flow field of the reheating furnace are estimated through the utilisation of a combustion model[8]. The turbulent model is employed to

simulate the turbulent characteristics of reactive flow involving combustible hot gases within a furnace[4].Table 1 summarises the various radiation transfer models used literature for modelling of reheating furnace using various commercial CFD softwares

2. CFD-Based Models: Exploring the Various Approaches:

- **Commercial Software Model Coupled with MATLAB (Model 1):** With the use of the commercial code FLUENT, the reheating furnace is represented in this model as a steady state radiating medium to compute the radiative heat flow. The conduction function uses the incoming radiation flux across slabs surface acquired from commercial programme FLUENT simulation as boundary condition.

$$\rho C \frac{\partial T}{\partial t} = \frac{\partial}{\partial x}\left(k \frac{\partial T}{\partial x}\right) + \frac{\partial}{\partial y}\left(k \frac{\partial T}{\partial y}\right) + \frac{\partial}{\partial z}\left(k \frac{\partial T}{\partial z}\right) \tag{1}$$

Table 1: Radiation Transfer Models in a Reheating Furnace Using Various Commercial CFD Softwares

Commercial CFD Package	Reheating Furnaces	Radiation Model (Heat Transfer, %)	Observations	References
FLUENT 3.2	WB furnace	P1 Radiation Model, (98.0%)	The experimental results and the expected distribution of temperature in slab and energy flow rates in the experimental furnace were in good	C Zhang et al. (1997) [10]
ANSYS Fluent 1.3	WB furnace	Discrete Ordinated (DO) Model (94.21%)	The furnace's energy efficiency is measured as a percentage of input energy used for slabs. Estimated figure of 37.7% is reasonably in line with actual value of 40.6%.	J.Gyu et. al. (2000) [11]
PHOENICS 3.1	Pusher-Type	Composite-Flux Radiation Model	A block wall installed in front of burners during the simulation gave the slab improved heating performance and decreased scale buildup risk near the bottom burner in the heating	Y. Tang et. al. (2002)
PHOENICS 3.1	Pusher-Type	Composite-Flux Radiation Model	According to the output of the numerical model, oxygen was dispersed evenly throughout except for areas near the burners. The projected value	Yong TANG, et al., 2003, [12]
STAR-CD	WB furnace	DO Model, (97.0%)	The findings reveal a 6.8% discrepancy between expected and measured heating	Chai et. al. (2008) [13]

STAR-CD	WB furnace	DO Model, (97.0%)	Only 3.7% of the measured furnace's heating efficiency differed from the projected heating efficiency.	Chia-Tsung Hsieh etal. (2008) [14]
ANSYS Fluent 10.0	WB furnace	DO Model (DO), (96.0%)	From the 27th slab location in the soaking zone, the skid mark severity decreased below 50K and was 37K at the time of exit.	Sang Heon et al. (2010) [15]
ANSYS Fluent 10.0	WB furnace	DO Model (97.0%)	At a throughput of 93.4 ton/hr, the energy absorbed by the steel slab is calculated to be 0.75 GJ/ton, which is close to 0.80 GJ/ton in everyday usage. Additionally, the slab's discharge temperature was	Sang Heon et al. (2012) [16]
ANSYS Fluent 12.0	WB furnace	DO Model	Heating process is significantly influenced by the slab charging temperature as section temperature difference and residence time decreases as charging temperature rises.	MingYan Gu et al. (2014) [17]
ANSYS Fluent 12.0	WB furnace	DO Model	For forecasting the transient heat transfer properties of slab, two alternative heat transfer models were contrasted. The highest temperature difference in the findings from two models is 2.24%, and calculation time for first model is 3hr and for the second model is 100. hr.	V. K. Sang et. al. (2015) [18]
ANSYS Fluent 12.0	WB furnace	DO Model (91.20%)	The outcomes of first model served as comparison point for second one. The mean slab temperatures at exit should fluctuate by ~3% according to simulations. The fastest model's computation time is ~5% of slowest model.	T.Morgado et. al. (2015) [6]
ANSYS Fluent 12.0	WB furnace	DO Model	When compared to the transient modelling method, the method reduces calculation time. Results from comparing a CFD simulation to a real instance were in conformation.	J. Manuel et. al. (2015) [19]

To determine the temperature profile of the slabs, a 3D transient heat conduction code for conductive heat flow within the slab was built in MATLAB [36][47]. Radiative boundary conditions are provided for the slab's whole perimeter. The boundary conditions for every slab face is determined by,

$$-k\left(\frac{\partial T}{\partial n}\right)_w = \varepsilon Q_{slab}^R - \varepsilon \sigma T_w^4 \tag{2}$$

The incident radiation flux is estimated from radiative heat transfer calculation that was calculated independently in reheat furnace (Q_{slab}^R). The outgoing radiative flux is represented by the second term. The conductive heat flux that was transmitted to slab through the surface is shown on the leftside. The border temperature and emissivity are T_w and ε, respectively, and the unit vector n, which extends from the boundary surface to the slab's interior, is normal to the boundary surface. This model has the benefit of being computationally affordable.

- **Commercial Software-Based Model (Model 2):** Similar to the second model, this particular model also utilises the commercial code FLUENT in order to conduct a three-dimensional numerical simulation of radiative heat transport within a water-based furnace. With the exception of the boundary condition specified in equation (2), which is deemed unnecessary due to the integration of both radiation and conduction models into a unified framework, the governing equations for this model remain identical to those of Model 2. The transient occurrence of slabs being periodically emitted into the rolling mill results in a brief phenomenon within the furnace. Due to its inherent limitations, the default function of FLUENT is unable to accommodate the phenomenon of slab movement. In order to replicate the oscillatory movement of slabs by transmitting temperature values across slabs at different intervals, a user-defined function (UDF) code, developed in the C programming language, is incorporated into FLUENT [20][21].

- **Commercial Software-Based Model (Model 3):** In Model 4, a skid support system is used to hold the slabs in place. As a direct consequence of this, the meshing procedure is significantly more difficult in contrast to model 3. It is necessary to cut the blocks in half along the perimeter of the skid support system. Model 4, which is quite identical to Model 3, also includes skid support systems for the slabs. These are the only differences between the two models. This change makes the model more complicated and significantly increases the amount of computational effort required to run it.

- **Commercial Software-Based Model (Model 4):** The present model incorporates an additional convection model and accounts for radiation within the furnace enclosure, which arises from the turbulent reactive flow of hot combustible gases through the burner intake. The skid support systems of Model 4 are additionally employed for the characterization of conduction within the slabs. The primary advantage of this model lies in its ability to replicate radiation, conduction, convection, and combustion phenomena through the utilisation of a unified code, hence enhancing its accessibility to users. The primary limitations of this model derive from its sophisticated skid support system design, which contributes to its overall complexity, and the

computational expense incurred by the inclusion of additional burner computations. The duration required to mimic the complete process exceeds 140 hours, which is a substantial increase compared to the aforementioned models[16][6]. The usual k-ε turbulence model used to simulate the WB furnace incorporates the consideration of density fluctuations through the application of Favre-averaging to the governing equations. Hence, the present simulation employs the energy and radiative transfer equations to solve the unsteady, Favre-averaged equations for continuity, momentum, turbulent kinetic energy (k), and eddy dissipation rate (ε).
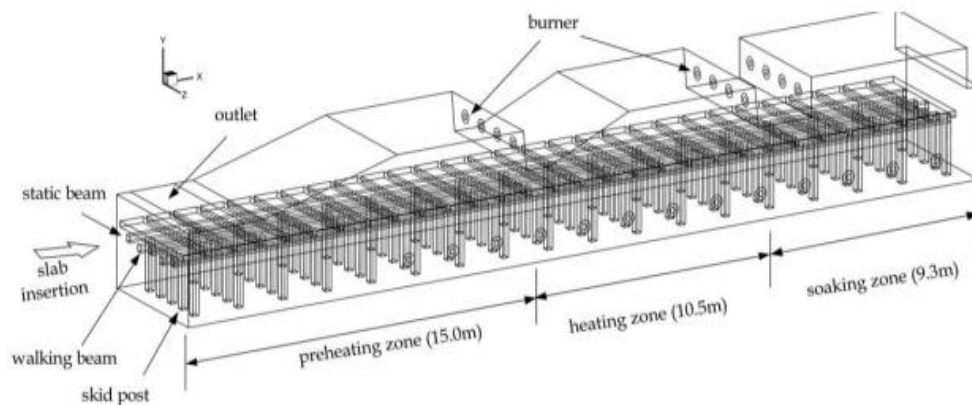
Figure 3: Configuration of the WB furnace, with axial and side burners in the upper and lower zones, respectively, on skid post and skid beam systems[16].
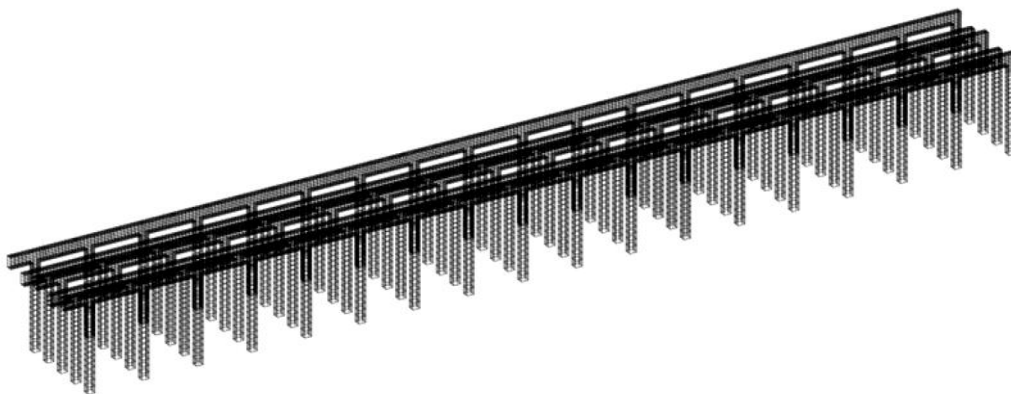
Figure 4: Mesh of skid post and skid beam systems[16]

3. Mathematical Formulation of CFD Models:

- **Flow and Energy Equations:** Since slabs are moved towards a rolling machine at specified intervals, the occurrences in the reheating furnace are intermittently transient. The equations governing the thermo-fluidic properties are unsteady, Favre-averaged continuity, momentum, energy, turbulent kinetic energy, and eddy dissipation rate equations are:

$$\frac{\delta(\bar{\rho})}{\delta t} + \frac{\delta \bar{\rho} \tilde{u}_j}{\delta x_j} = 0$$

(3)

$$\frac{\delta(\bar{\rho} \tilde{u}_i)}{\delta t} + \frac{\delta \bar{\rho} \tilde{u}_j \tilde{u}_i}{\delta x_j} = \frac{\delta}{\delta x_j} \left[\mu \left(\frac{\delta \tilde{u}_i}{\delta x_j} + \frac{\delta \tilde{u}_j}{\delta x_i} \right) - \frac{2}{3} \mu \frac{\delta \tilde{u}_k}{\delta x_k} \right] - \frac{\delta \bar{p}}{\delta x_i} + \frac{\delta(-\overline{\rho u''_i u''_j})}{\delta x_j}$$

(4)

$$\frac{\delta(\bar{\rho} \tilde{\hbar})}{\delta t} + \frac{\delta \bar{\rho} \tilde{u}_j \tilde{\hbar}}{\delta x_j} = \frac{\delta}{\delta x_j} \left(\frac{\mu_t}{\sigma_\hbar} \frac{\delta \tilde{\hbar}}{\delta x_j} \right) + \tilde{S}_\hbar$$

(5)

Where, μ, t, u, h and p are dynamic viscosity, time, velocity component, particular pressure and enthalpy, respectively [61]. To determine k and ε, following transport equations are solved.

$$\frac{\delta(\bar{\rho} \tilde{k})}{\delta t} + \frac{\delta \bar{\rho} \tilde{u}_j \tilde{k}}{\delta x_j} = \frac{\delta}{\delta x_j} \left[\left(\mu + \frac{\mu_t}{\sigma_k} \right) \frac{\delta \tilde{k}}{\delta x_j} \right] - \overline{\rho u''_i u''_j} \frac{\delta \tilde{u}_j}{\delta x_i} - \bar{\rho} \tilde{\varepsilon}$$

(6)

$$\frac{\delta(\bar{\rho} \tilde{\varepsilon})}{\delta t} + \frac{\delta \bar{\rho} \tilde{u}_j \tilde{\varepsilon}}{\delta x_j} = \frac{\delta}{\delta x_j} \left[\left(\mu + \frac{\mu_t}{\sigma_\varepsilon} \right) \frac{\delta \tilde{\varepsilon}}{\delta x_j} \right] - C_{1\varepsilon} \frac{\tilde{\varepsilon}}{\tilde{k}} \left(\overline{\rho u''_i u''_j} \frac{\delta \tilde{u}_j}{\delta x_i} \right) - C_{2\varepsilon} \bar{\rho} \frac{\tilde{\varepsilon}^2}{\tilde{k}}$$

(7)

When all chemical species have Lewis numbers of unity and low mach numbers, specific enthalpy of mixture is computed as,

$$\tilde{\hbar} = \sum_k \tilde{Y}_k \int_{T_{ref}}^{T} C_{p,k} dT$$

(8)

Calculating the turbulent viscosity is as follows:

$$\mu_t = \bar{\rho} C_\mu \frac{\tilde{k}^2}{\tilde{\varepsilon}}$$

(9)

For turbulence closure, the realisable k-ε turbulence model [62] was employed; the Reynolds stress term was modelled as follows:

$$\overline{\rho u''_i u''_j} = \mu_t \left(\frac{\delta \tilde{u}_i}{\delta x_j} + \frac{\delta \tilde{u}_j}{\delta x_i} \right) - \frac{2}{3} \left(\mu_t \frac{\delta \tilde{u}_k}{\delta x_k} + \bar{\rho} \tilde{k} \right) \delta_{ij}$$

(10)

The time-average value is denoted by the superscript $(-)$, while the Favre-average is denoted by the tilde ($\sim$). The source term ($\tilde{S}_\hbar$) contains heat produced by chemical reactions and divergence of radiation flux. The superscript (") denotes variance of the Favre-average. C_{1e}, C_{2e} C_μ, σ_h, σ_k and σ_e are the model parameters; their respective constant values are 1.44, 1.92, 0.09, 0.9, 1.0, and 1.3 [22].

- **Turbulent Combustion Model:** The chemical composition and temperature distribution in reheating furnaces are forecasted using a combustion model. The instant thermochemical state of fluid is connected to a conserved scalar variable known as the mixing fraction, f, which is represented as [23][24],

$$f = \frac{Z_k - Z_{k,ox}}{Z_{k,fuel} - Z_{k,ox}}$$

(11)

Where, Z_k represents the element's mass fraction. Subscripts *ox* and *fuel* denote values at oxidizer stream inlet and fuel stream inlet respectively. The Favre-averaged mean and variance of f have the conserved equation expressed as

$$\frac{\delta(\bar{\rho}\tilde{f})}{\delta t} + \frac{\delta\bar{\rho}\tilde{u}_j\tilde{f}}{\delta x_j} = \frac{\delta}{\delta x_j}\left(\frac{\mu_t}{\sigma_t}\frac{\delta\tilde{f}}{\delta x_j}\right) \tag{12}$$

$$\frac{\delta(\bar{\rho}\tilde{f}''^2)}{\delta t} + \frac{\delta\bar{\rho}\tilde{u}_j\tilde{f}''^2}{\delta x_j} = \frac{\delta}{\delta x_j}\left(\frac{\mu_t}{\sigma_t}\frac{\delta\tilde{f}''^2}{\delta x_j}\right) - C_g\mu_t\left(\frac{\delta\tilde{f}}{\delta x_i}\right)^2 - C_d\bar{\rho}\frac{\tilde{k}}{\tilde{\varepsilon}}\tilde{f}''^2 \tag{13}$$

where, constants σ_t, C_g, and C_d have value 0.7, 2.86, and 2.0, respectively [25]. It is then followed by computation of instantaneous values of species mass fraction, density, and temperature as,

$$\tilde{\phi} = \int_0^1 P(f)\phi(f)df \tag{14}$$

where $P(f)$ is assumed β function characterized by $\tilde{f}$ and $\bar{f}''^2$ [25].

- **Radiation Heat Transfer Model:** The radiation intensity at any position $\vec{r}$ along a path $\vec{s}$ through an absorbing, emitting, and non-scattering medium is given by [26]

$$\frac{dI(\vec{r},\vec{s})}{ds} = -\kappa I(\vec{r},\vec{s}) + \kappa I_b(\vec{r}) \tag{15}$$

Where, I, I_b, and κ are intensity, black-body intensity and absorption coefficient respectively. One factor that influences black body intensity is the local temperature. Divergence of the radiative heat flux is one way that radiation's impact on the energy equation is expressed,

$$-\Delta \cdot q^R = \kappa\left(4\pi I_b(\vec{r}) - \int_{4\pi} I(\vec{r},\vec{s})d\Omega\right) \tag{16}$$

- **Radiation Boundary Condition:** A diffusely emitting and reflecting wall to specifying slab surface and furnace walls is bounded by,

$$I(\vec{r}_w,\vec{s}) = \varepsilon_w I_{bw}(\vec{r}_w) + \frac{1-\varepsilon_w}{\pi}\int_{\vec{s}'\cdot\vec{n}_w<0} I(\vec{r}_w,\vec{s})\left|\vec{s}\cdot\vec{n}_w\right|d\Omega' \tag{17}$$

Where, $\vec{n}_w$ is unit normal vector and ε_w is furnace wall emissivity. The aforementioned equation shows that total intensity at surface is sum of the intensities that are both emitted and reflected. Burner inlets and stack outlets are regarded as if they were black body walls for radiation boundary conditions, $\varepsilon_i = 1.0$.

4. **CFD based Modelling:** Yang presented a technique for transiently heating slabs in industrial type continuous reheat furnace based on CFD simulation. To achieve a consistent temperature distribution across the slab, they used low Reynolds number (Re) turbulent models in conjunction with a second order convection scheme and a radiation

model for gaseous flow. Lagrangian frame of reference was utilised to track the movement of each slab and its temperature progression, while Eulerian frame of reference was used to track the distribution of slab temperatures. demonstrated simulation showed, under pseudo-steady state operation, both temperature profiles correspond. Using a general-purpose CFD programme, the slab motion and transient heating was simulated forslab reheat furnace usingPHEONICS3.2. The generalised governing partial differential equation have been used to simulate turbulent gas flow, convection, conduction, and radiation heat transfer, as well as transport phenomena[27].

$$\frac{\partial}{\partial t}(\rho\phi) + div(\rho u\phi) = div\big(\Gamma_{\phi,eff}\, grad\phi\big) + S_\phi \tag{18}$$

Where, ϕ stands for the common flow variables, such as the velocity, temperature, k and ε. The fluid's density and velocity vector are both represented by the symbols u and. The effective exchange coefficient, or S, is a common source term for flow variables and is created by adding the exchange coefficients for turbulent and laminar flow [30]. By resolving temperature and heat flow on slab surface simultaneously, Huang et al. used coupled simulation approaches to create a uniform temperature distribution across the slabs. Huang used the commercial programme STAR-CD to research a 3D simulation approach of a WB furnace based on turbulent reactive flow and heat transfer in the furnace to arrive at a steady state solution. They modelled slabs as a very highly viscous, uniformly flowing laminar fluid. The temperature, heat flow on the slab surface, and skid mark effect were all accurately estimated. They discovered that the primary reason of the skid effect on the slabs is radiative shielding by static beam[28].

The methods to determine the temperature variation inside slabs and gas combination using a coupled solution method were developed by Hsieh et al. Due to the radiation shielding effect of static beams and the water cooling system, they also measured the skid mark. Improved skid button geometry helps to lessen the skid mark effect. Using the commercial software STAR-CD, they introduced coupled model to solve the temperature and heat flux over slab in the furnace enclosure. To lessen the radiation shielding effect, they raised the skid button's height[13].In order to forecast the heat transfer to slab in a continuous reheating furnace, Venturino et al. devised a new methodology. The temperature inside the slab was determined using a numerical method, coupled methodology, and commercial software FLUENT to identify the thermal radiation inside the furnace using typical CFD techniques [29]. They demonstrated the benefit of his linked model by comparing the findings of his conduction model with an analytical solution.

The whole coupled technique can be developed much more quickly if a specific module is coupled to a commercial CFD software [26]. The temperature variation of the slab in the reheating furnace is solved using full coupled CFD approaches for radiative heat transfer in reheating furnace and conduction model. The Navier-Stokes equations are resolved using the commercial CFD code utilising the finite volume formulation and pressure correction approach. Standard k-ε turbulence model and discrete transfer model are used to model turbulent reactive flow for eddy-break combustion. The reheating furnace's radiative heat transfer is simulated using a radiation model [29].

$$\rho C \frac{\partial}{\partial t}(T) = \frac{\partial}{\partial \xi_j}\left(Jk g^{jk} \frac{\partial T}{\partial \xi_k}\right) + JS(\xi\eta\varsigma) \tag{19}$$

Where, J is the Jacobian determinant of coordinate transformation and g^{ij} stands for the contravariant metric tensor components. With a second order fully implicit first order accurate scheme, the spatial and temporal discretization methods are applied, respectively. A TDMA and a block correction technique served as the foundation for the solution process. To solve the discretized equations, Dirichlet and non-Dirichlet type boundary conditions are employed [29].
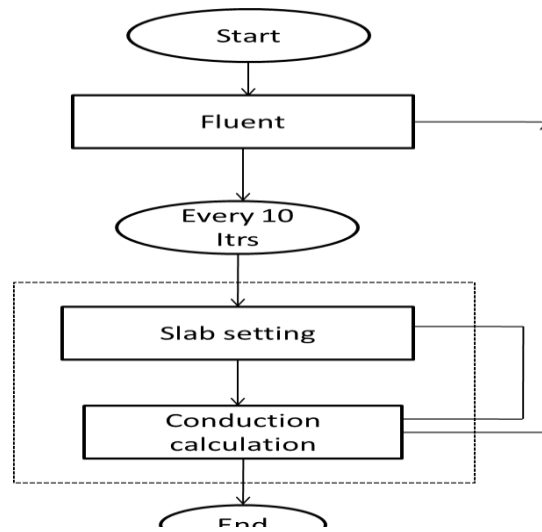
Figure 5: Flow chart for slab temperature calculation scheme for a coupled fluid flow and [29]

The mathematical simulation of a regenerative slab reheat furnace was described by Zhang et al. With the use of the software programme FLUENT, they recreated turbulent non-premixed combustion. By resolving the modified conduction equation, the slab's movement is represented[10].

$$\frac{\partial}{\partial x_i}\left(\rho_s u_{i,s} C_{ps} T_s\right) = \frac{\partial}{\partial x_i}\left(\lambda_s \frac{\partial T_s}{\partial x_i}\right) \tag{20}$$

Where, thermal conductivity and specific heat are represented by λ and C, respectively, while the moving slab's characteristics are indicated by the subscript *s*.

In a WB furnace, Kim et al. examined computational methods to analyse the turbulent reactive flow and radiation heat transfer. With aid of FLUENT, they carried out 3D analysis with the basic burner, simulating the analysis of heat transfer under steady state conditions, and quantitatively comprehending the intricacy of combustion process and heat transfer characteristics in the type of furnace [28].

For a large reheating furnace, Yukun Hu et al. (2015) created a hybrid transient mathematical model by securely fusing the zone approach with CFD. The constructed model has the whole energy balance derived from fundamental principles, which makes it

easier to assess the furnace's individual fuel usage and efficiency. The mathematical model outperformed the semi-empirical level-2 model employed in the plant by reducing the run time by 170 times for a large reheating furnace. The model was still able to reasonably forecast the furnace's overall thermal behaviour [30].

A unique approach to resolving the PDE optimum control problem was put forth by Yang Zhi et al. To obtain the reference values for the idealistic furnace zone temperatures and idealistic slab temperature variation in a steadystate operation, they added the adjoint problem to the optimisation model. Based on according to a comparison between the mathematical model and experimental results,the current heat transfer model performed well for estimation of thermal behaviour around a slab [31].

S. Chakraborty et al. (2017) used ANSYS Fluent 15.0 and a custom 3D transient code to simulate the fluid flow and heat transfer within a pusher type reheating furnace for steel billets with coal burners. They used an iterative simulation process to study the heat diffusion in regularly moving billets that were modelled using coupled simulations. With good accuracy and reasonable processing time, the highly nonlinear DPM of coal particle problem, its homogeneous and heterogeneous responses, and its periodic transient nature were successfully handled. The proposed model allowed for a 60% reduction in calculation time compared to the entire transient discrete phase combustion model with periodic motion of billets [32].

To simulate the flow behaviour, combustion, and multiscale heat transfer inside the reheating furnace, Guangwu Tang et al. (2018) created a 3D CFD model. To simulate particular slab walking speeds, a dynamic mesh model with ANSYS Fluent and a UDF was examined. Also taken into consideration were fuel differences over time in various zones. The instrumented slab trials performed in the SSAB Mobile mill served as a validation test for the model [33].

A method to derive the boundary conditions for slab model from a steady state model of furnace was presented by Z. Ahmed et al. in 2019. To create a computationally less expensive model, they obtained the radiation and convection heat fluxes using a steady-state model. When the temperatures from the CFD model and thermocouple data within the furnace were compared, they agreed well[34].

In order to simulate the gas circulation, heat transfer, and slab heating process for a WB furnace, which is influenced by a number of variables, including gas velocity, slab speed, and the height and spacing of the burners, Yiwei Liu (2020) developed a geometry model. By taking into account the slab movement utilising unsteady simulations and a self-created computational algorithm, the properties of slab heating were investigated. All of the simulations were completed using scheme instructions connected to the programme ANSYS FLUENT 16.2. The results demonstrate that the inner air flow's entrainment effect increases the flames' coverage area and raises the slab temperature throughout the entire furnace by more than 28.5% [35].

III. ANALYSIS OF REAL AND SIMPLIFIED BURNERS

The real burner has an intricate geometry with numerous air inlets, but the simplified (or basic) burner just has one air inlet. This is where the real burner differs from the simplified burner. As can be seen from figure6, the basic burner is computationally cheap and produces results that are in good conformation with temperature and axial velocity along the axis. The air and fuel flow rates are identical to those of the actual burner [11]. The temperature distribution of the upper and lower parts of the furnace are shown in figure7, which also compares the outcomes of simulations and measurements. In both instances, it was found that the upper zone of furnace has a higher temperature than lower zone [11].
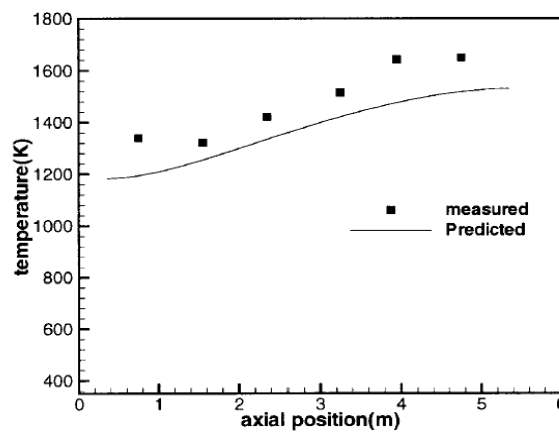
Figure 6: Comparison between measured and predicted temperatures in simplified burner [11]
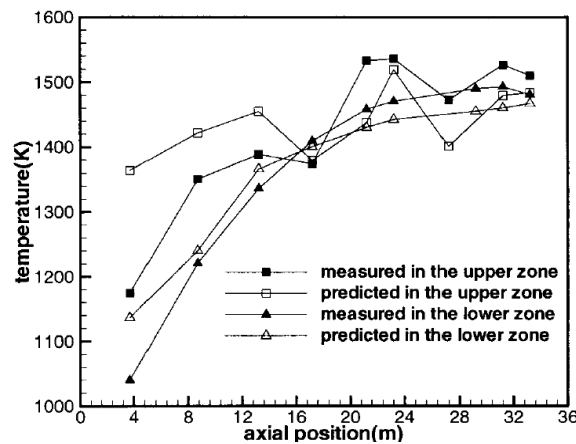
Figure 7: Experimental and simulated temperature in upper and lower zones of furnace along its length [11]

The distribution of temperature and the pattern of hot gas flow in the furnace were both significantly predicted by CFD. To model the 3D turbulent flow field and get the uniform homogenous temperature distribution in slabs at the exit of the reheat furnace, Tang et al. employed the PHOENICS 3.1. The momentum, combustion, and radiation models were combined in the current calculation. To improve the heating efficiency and lessen the

likelihood of scale formation near lower burner in heating zone, they simulated the velocity flow field of hot combustible gases with and without the inclusion of a block wall in front of burner. They also noticed a change in the gas flow pattern when a block wall was present [36].
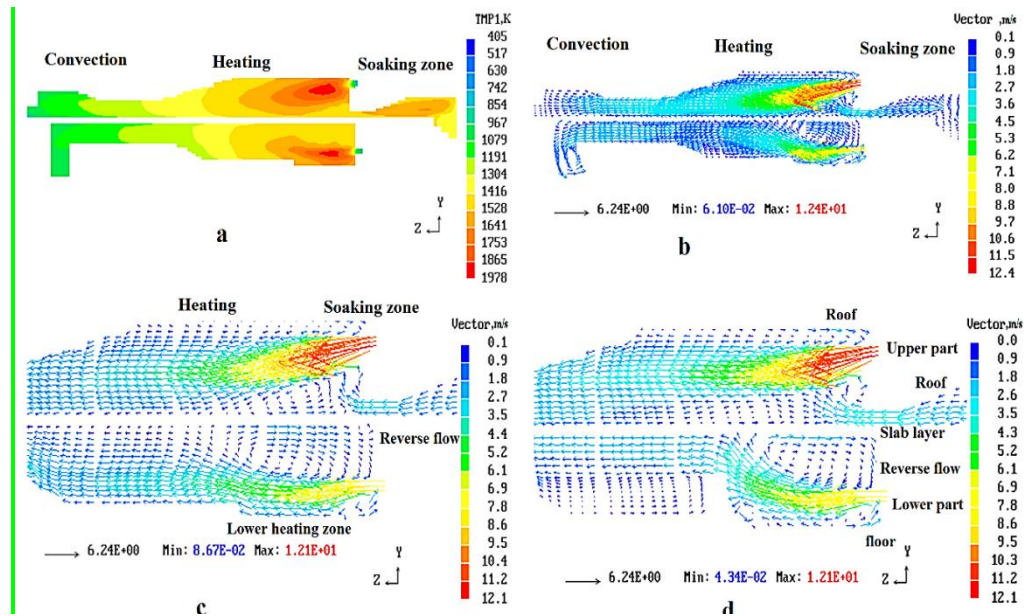

Figure 8: (a) Gas temperature variation, and (b) hot gaseous flow pattern in longitudinal direction; and velocity variation of gaseous flow near burner in heating and soaking zone of the (c) without and (d) with block wall[36]

Tang et al. further simulated fluid flow, turbulent combustion, and radiation in a linked way and defined the flow distribution in the furnace enclosure to forecast the gas flow in pusher type reheating furnace. To simulate the 3D turbulent flow field, they employed the commercial CFD code PHOENICS 3.1 [12].Using the commercial programme STAR-CD, Hsieh et al. effectively calculated the 3D turbulent reactive flow of combustible gases and radiation heat transfer inside furnace. They used the entire WB furnace as a domain to assess the effectiveness of the heating and the uniformity of temperature distribution within slabs. They discovered that WB furnace type system, not only induces radiative shielding but also modifies the flow of combustion gases and influences radiative heat transfer from combustion gases and furnace walls to the bottom portion of slab surface; and is primary cause of the skid marks on the bottom surface of slabs. As a result, the impact of cooling water on the slabs' bottom-most portion's heating efficiency is minimal [14].

With the aid of the commercial programme STAR-CD, Hsieh et al. later calculated a 3D turbulent reactive flow and radiation heat transfer in a slab reheat furnace that uses a WB furnace design. They used the same geometry as a real furnace and placed all of the reheat furnace's elements on his domain. They then solved the problem in a pair of ways. They believed the slabs to be an extremely viscous fluid travelling continuously around the furnace. They made use of the Favre averaged high Reynolds number k-ε turbulence model of the governing equations. They observed that the walking beam system is the primary factor contributing to radiation shielding, resulting in the formation of skid marks [13].
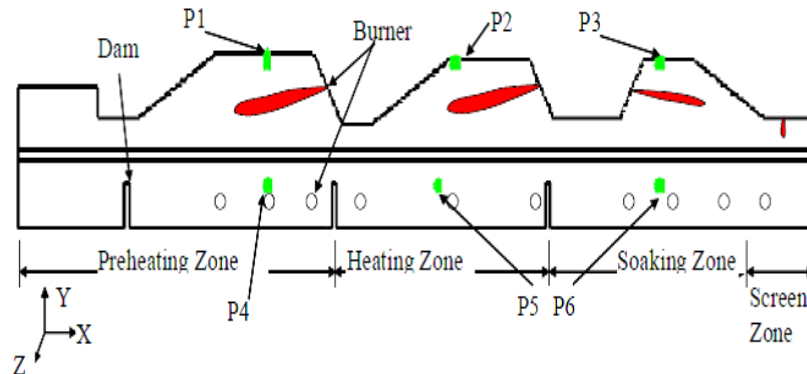
Figure 9: Schematic of WB Furnace Showing Temperature Measurement Points(P_i)[13]

Table 2: Temperature Comparison between Experimental and Estimated Temperatures at Six Locations[13]

Measurement Point (P_i)	1	2	3	4	5	6
Experimental	1266.0	1504.0	1451.0	1335.0	1478.0	1445.0
Predicted	1240.0	1449.0	1365.0	1245.0	1301.0	1369.0
Error (%)	2.05	3.59	5.92	6.74	11.97	5.25
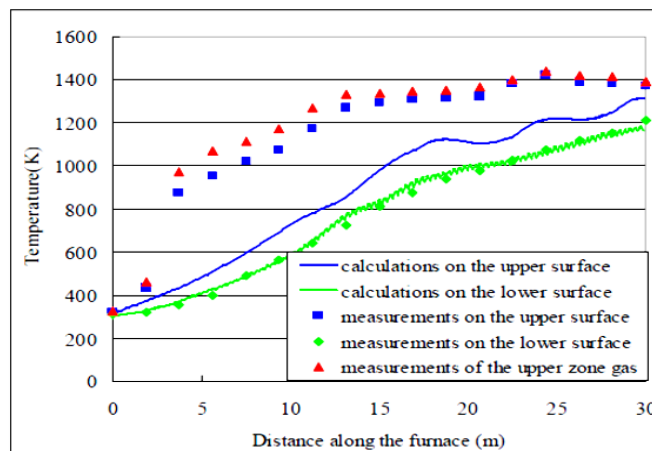
Figure 10: Temperature variation along central lines on top and bottom surfaces of slab [13]

In their study, Han et al. employed the commercially available software FLUENT to conduct an unstable computation with the objective of obtaining a periodically transient solution. In addition, the researchers integrated a skid post and beam arrangement into their model, as this particular design has the potential to impede heat conduction and consequently impact the heating characteristics of the slabs. The user-defined function (UDF) facilitates the movement of slabs in a specified direction. The study investigated the heating characteristics of a slab within a furnace through unsteady calculations. Additionally, the research analysed the thermal efficiency of the furnace and the thermofluidic properties of the gaseous phase. Upon the culmination of the slab's journey, there was a reduction in the intensity of the skid marks to a value of 37K[15].
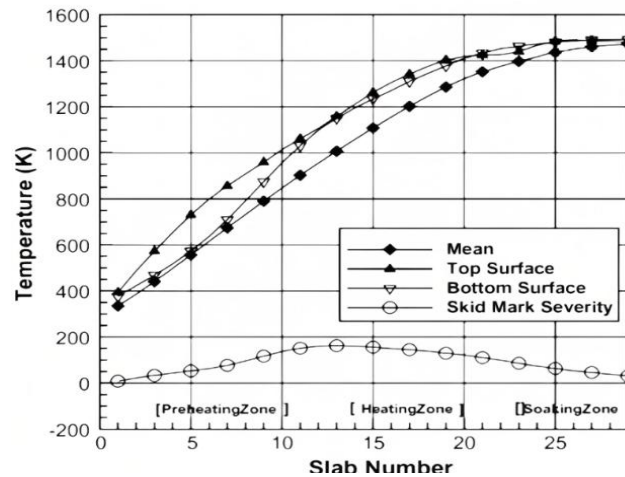
Figure 11: Temperature profiles of slab and skid mark severity [15]

The certainty of uneven temperature distribution on lower part of slab, which is brought on by obstruction of radiative heat transmission, is embodied by the severity of the skid mark. It is calculated using the difference between average temperature at contact points and bottom surface of slab. According to figure11, the slab's skid mark severity is at its peak in heating zone, between the 13th and 15th slab positions, and gradually decreases as it moves into soaking zone. The skid mark severity starts out at 100 K, drops to 50 K at the 27th slab, and then ultimately drops to 37 K at the moment of exit [15].Using UDF and FLUENT, Han et al. explored the unsteady numerical simulation of a WB furnace. When the slab emission temperature to the rolling mill is between 1373K and 1573K, they were able to determine optimum residence duration of reheating furnace to maximise its efficiency and reduce fuel consumption. The following formula is used to determine how well the WB furnace performs [16].

$$\text{Performance} = \frac{\text{Heat required for slab heating}}{\text{Total heat input}} \times 100 \tag{21}$$

Table3: Optimal Characteristics of the WB Furnace at end of Furnace of 27th Position of Slab[16]

Residence Time (s)	6033.0	6497.0	6961.0	7425.0	7889.0
Slab Mean Temperature	1251.0	1301.0	1362.0	1424.0	1449.0
Slab Mean Heat	35381.0	34814.0	34251.0	33656.0	33025.0
Furnace Efficiency (%)	49.49	45.21	44.41	43.72	42.91
Severity of Skid Mark	55.0	50.0	40.0	35.0	30.0

Due to the large temperature difference between the slabs and combustible gases, a low residence period can encourage a higher heat flux. Additionally, it may increase the thermal gradient of the slabs and the temperature at which skid marks become more severe [16].With the aid of the commercial programme FLUENT, Gu et al. suggested a way to obtain slab reheating process in a regenerative WB furnace by matching boundary conditions of furnace with burner characteristics, and by taking into account the regenerative reversing combustion process and slab motion [17]. The resultant simulation findings were found to be in conformation with experimental data, as can be shown in figure12 (a). When comparing

the centre temperature of the upper surface, they discovered a 1.59% relative inaccuracy between the experimental and simulated data. It can be seen that this paper's methodology is workable and that the outcomes are attainable [17]. At charging temperatures of 30°C, 400°C, and 500°C, figure12(b) illustrates the impact of lower slab temperature. It has been shown that varying the slab charging temperatures increased the heating property of the slabs and affected how long they took to heat up. The slab reaches its lowest temperature (1223.7°C) at room temperature in just 221 minutes. Heating time reduced from 186.6 minutes to 184 minutes as the charging temperature rose from 400°C to 500°C, which is 37 minutes less time than charging at 30°C [17].
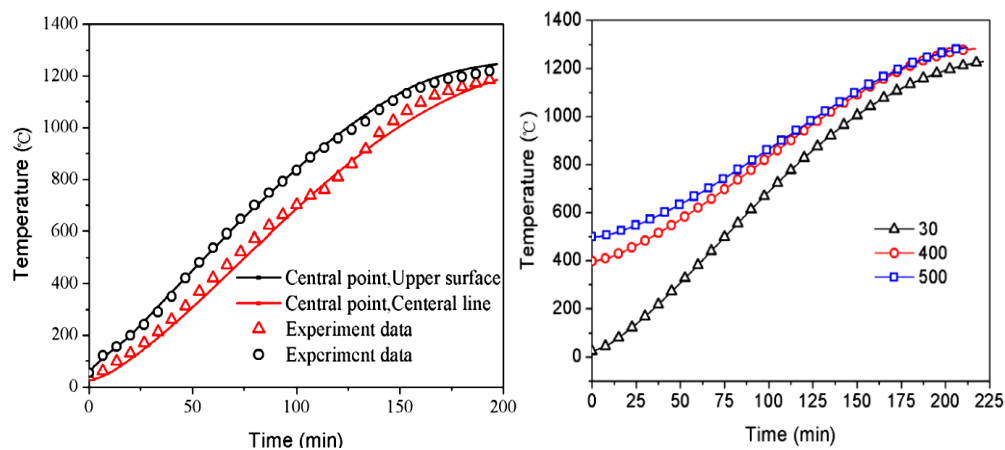

Figure 12: (a) Slab surface and central line temperature (b) Influence of slab lower temperature on different charging temperatures[17]

In terms of computing speed and accuracy, Singh et al. examined two distinct models. The model A is based on a radiationactive medium, and the steady state heat transfer inside the furnace is carried out using FLUENT, while the transient conduction inside the slab with a radiation flux boundary condition on slab surface is resolved using custom MATLAB code. Without utilising any experimental data, the model B is a turbulent reactive flow with combustion model using software ANSYS FLUENT. Because slab movement is a recurring transient phenomenon, FLUENT's default function is unable to handle slab movement, so a UDF is used. As a result, two transient simulations are run: the first simulates radiative heat transfer inside the reheat furnace while the second simulates conduction in slabs with periodic transient motion. They noticed that the largest temperature difference was 2.25 percent and that the computing times for the first and second models were 3 hours and 100 hours, respectively. [18].

Figure 13(a) and 13(b) demonstrate the conformation between the two models. The top and bottom surfaces' area-averaged temperatures show a maximum temperature difference of 1.64% and 0.11%, respectively, between the two models [36]. As shown in Fig. 43, volume-averaged temperature of slab rises as slab emissivity rises from 0.3 to 1.0 because slabs may absorb more radiation from the furnace gas as surface turns black, but the final temperature fluctuates relatively little at the end of slab departure [18].
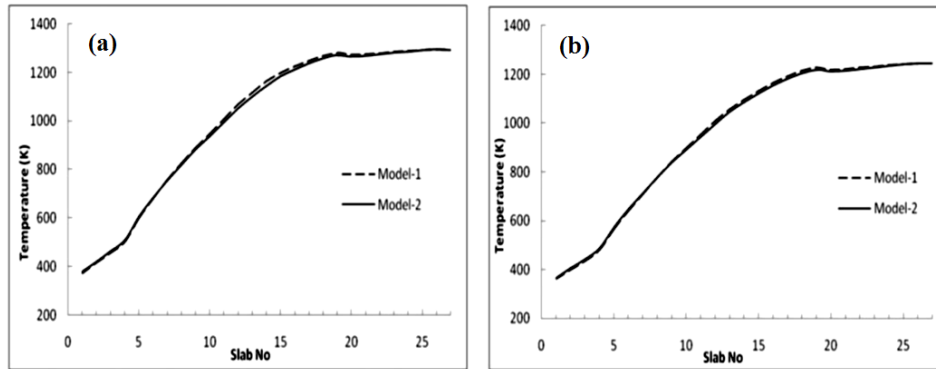
Figure 13: Valuation of area-averaged (a) top, and (b) bottom surface temperature of 14th slab in between modelA and modelB[18]
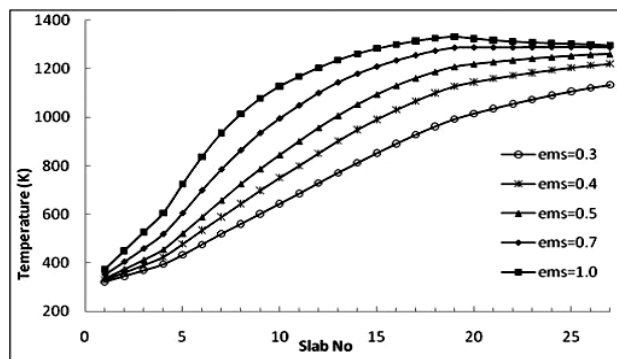
Figure 14: Slab emissivity's effect on the volume-averaged temperature of the slabs with constant furnace medium absorption coefficient (1.0 m^{-1}) and furnace wall emissivity (0.75) [18]

Morgado et al. developed a numerical model to simulate the heating of steel slabs in reheating furnace with a WB furnace design. They used FLUENT to execute unsteady computation of the slab heating and successfully implemented the periodic motion of the slabs using a UDF as FLUENT is compatible with a UDF that was built in C language to carry out this action. By transferring the entire temperature profile of one slab to next adjacent slab and assuming that slabs move instantly and don't disrupt the surrounding flowing fluid, the motion of the slabs is mimicked. The first model (model I) is based on heat conduction simulations of turbulent reactive flow in a WB furnace. The other one (model II) is merely based on the zone approach; the first model obtains the average temperatures and chemical compositions for each zone. The mean slab temperature at the end of the slab exit was only 3% different between the two models when they compared them based on thermochemical composition, while the quickest model (the zone-based model) only took 5% longer to compute than the slower one [6].
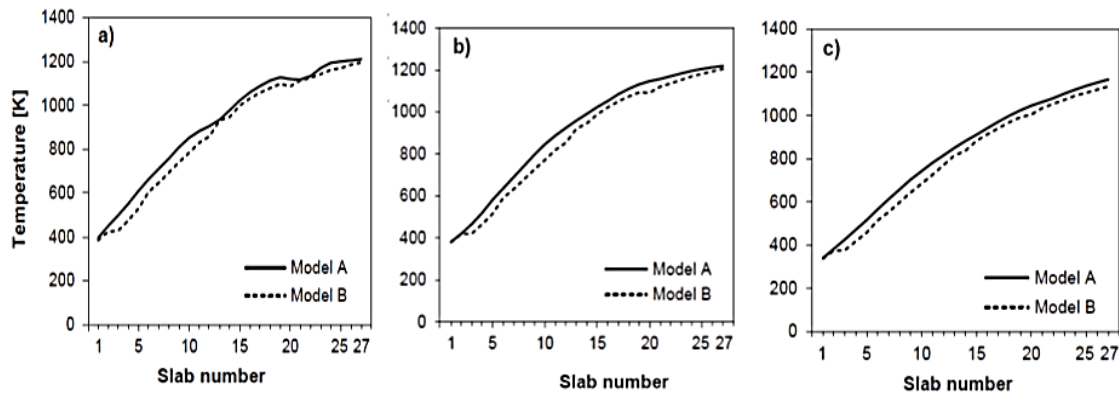
Figure 15: Assessment of mean temperature of slabs in model A and B. (a) top surface, (b) bottom surface and (c) volume averaged temperature[6].

As depicted in Figure 15, both Model I and Model II present the average slab temperature. The reduced heat flux in model B significantly affects the preheating zone, resulting in a consistently lower predicted mean temperature of the slabs along the length of the furnace compared to model I. However, the discrepancy among volume-averaged temperatures is less than 3%. Ultimately, it has been ascertained that model II is capable of effectively estimating the temperature profile of slabs within a reheating furnace, while simultaneously necessitating a substantial decrease in computational effort[6].

Figure 16(a) and 16(b) show that as the slabs' emissivity and residence time are increased, the mean temperature of slabs gradually rises along the length of WB furnace [37]. In comparison to the transient modelling method, Casal et al.'s novel methodology required less computation time to simulate a reheating furnace in steady state conditions. They altered the energy transport equation to carry out the billet movement. They added an ad-hoc process that was programmed as a user-defined function to the commercial code language to replicate the passage of the billets from one stage to next level [19].
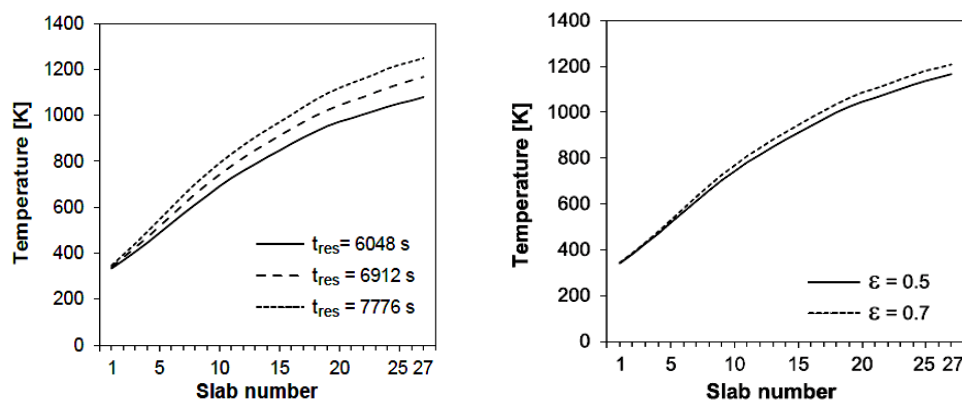
Figure 16: Influence of(a) residence time and (b) slab emissivity on slab's average temperature profile along length of reheating furnace[6].

IV. MONTE CARLO SIMULATION

1. **Previous Studies:** Through the use of an advanced computer control system, Yang and a colleague created a dynamic model to determine the temperature profile of each slab in a continuous pusher type reheating furnace. Partial differential equations served as the foundation for this discrete dynamic state space mathematical model. The dynamic interaction between temperature profile of slabs in furnace is provided by the global system modelling. Computer simulation was used to study this process and make it more energy-efficient. The temperature distribution of the slabs is determined using a modified heat conduction equation, and moving condition of the slabs in the reheating furnace is modelled using an additional factor [37].

$$\rho C \frac{\partial T(x,y,t)}{\partial t} = \left[\frac{\partial}{\partial x}\left(k_s \frac{\partial T}{\partial x} \right) + \frac{\partial}{\partial y}\left(k_y \frac{\partial T}{\partial y} \right) \right] - v(t) \frac{\partial T(x,y,t)}{\partial y}$$
(22)

An enormous amount of energy is utilised in reheating furnace to heat the slabs to the ideal temperature. Yang and Lu conducted more research, using a dynamic model to determine the best furnace zone temperature and set point for low energy usage under varied operating scenarios. Reduced energy use and improved heating slab quality led to significant economic advantage when the simulation ran effectively for more than a year [38].

It is generally recognised that energy usage, production costs, and equipment upkeep are all intimately correlated with the temperature controls of the slabs in WB furnace. Chen et al. conducted an extensive study on the energy consumption, heat balance, energy recovery, and performance of reheating furnaces. They concentrated more on reheating furnace's efficiency in terms of input energy, including sensible energy, fuel combustion energy, and slab size[39].Based on the heat balance of furnaces, empirical evidence reveals that energy recovery from hot flue gases has significant role in energy management, contributing 15.7% of the input energy. The efficiency corresponding to the basis of input energy and slab size during the analysis period are 41.74% and 59.34%, respectively [75].

The imperial relationship, which is dependent on the heating curve, was used to manage the production rate of the reheat furnace. In a hot strip mill, an arctangent function represents a typical heating curve (eq. 52) while a sinusoidal curve represents a high yield (eq. 53). Moreover, the second order polynomial curve indicates a poor production rate (eq. 54). By using 2D diffusion equation and the finite difference approach with a second order central difference and fully implicit scheme, the temperature distribution of slab is computed[39].

$$\frac{T_s - T_c}{T_d - T_c} = 0.5 + 0.475 Arc\,tan\left[1.75\left(2\frac{z}{L} - 1 \right) \right] \tag{23}$$

$$\frac{T_s - T_c}{T_d - T_c} = sin\left(\frac{z}{L} \right) \tag{24}$$

$$\frac{T_s - T_c}{T_d - T_c} = \left(\frac{z}{L}\right)^2 \tag{25}$$

Where, z, T_s, T_c and T_d are slab location in the furnace, slab surface temperature, charging temperature, and discharging temperature respectively.
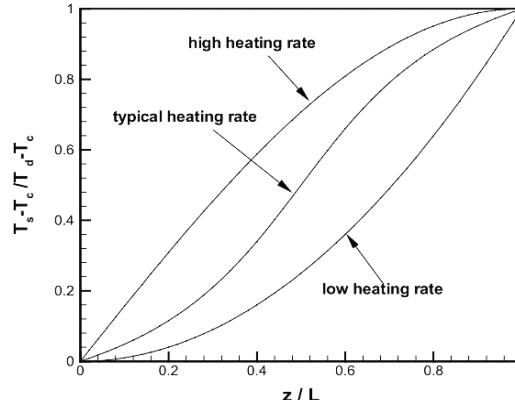

Figure 17: Typical Perspective of the Reheating Furnace and Temperature Distribution[39]

The distance between billets and the rate of movement of the walking billets both have an impact on the productivity of the WB furnace. To determine the ideal spacing between the billets, Jaklic et al. produced productivity curve utilising various charging spaces between the billets for various billet sizes. However, the three-temperature model is used to obtain heat exchange between combustible gas in the reheat furnace, the furnace wall, and surface of the billets[40]. He conducted additional research to create a simulation model based on Monte Carlo approach to determine slabs' heating properties in a pusher type reheating furnace. To solve the radiation transport in the furnace enclosure, view factor matrix is determined using Monte Carlo approach [41].

$$F_{i \to j} = \lim_{N_i \to \infty} \left(\frac{N_{i \to j}}{N_i}\right) \approx \left(\frac{N_{i \to j}}{N_i}\right)_{N_i \gg 1} \tag{26}$$

The heating characteristics of slabs in reheating furnaces are influenced by a number of factors, including the location of the slabs, their thermo-physical characteristics, the type of burners used, the fuel used, how the burners are arranged in the top and lower portions of the furnace, and the design of the furnace [76]. Han et al. created the experiment initially on a bench-scale reheating furnace to look into the slabs' heating properties. This model simulates the same conditions as actual reheating furnaces and is an identical replica of those furnaces. The projected findings are in good conformation with the experimental results after they built code to measure the temperature of slabs and furnace gases[42].

To study radiative heat transport inside the furnace, numerous techniques have been found and created. One of them can be resolved using the DO method along with energy-balanced equations that include radiative heat transfer (RTE) as a source term. In order to determine the design and operational characteristics of a continuous reheating furnace, Safari et al. created a mathematical model based on the Monte Carlo approach.

Using discrete photons, the Monte Carlo approach tracks the photons until they are absorbed by the gas or any surfaces inside the furnace enclosure. Additionally, it was found that as furnace height climbed from 0.6 to 1, fluctuation in slab temperature dropped from 1260 °C to 1096 °C, indicating a 13% reduction in furnace efficiency. When the slab's emissivity is increased from 0.1 to 1, a 54% improvement in efficiency, the slab's temperature similarly rises from 1026 to 1582°C [77]. The 3D finite difference approach is used to determine the slab's temperature distribution. The model reads the data from the view factor matrix at the start of simulation. Heat balance is used to determine the temperature of the furnace floor parts. Additionally, a GUI was used to portray the simulation model in a user-friendly manner [43].

The Monte-Carlo Integral approach was put forth by W. Zhou et al. (2015) for calculating the direct exchange area. Complex geometry zone problems and self-zone radiation problem were both solved using the zone method with an updated Monte Carlo Integral. The industrial furnace's radiation transport was modelled and simulated using it. The simulation's output was compared to actual industrial data, which revealed excellent agreement and demonstrated that the zone approach was thorough and simple to use for radiative phenomena in the furnace [44].

A strategy framework for the best reheating procedure for large-scale furnaces utilising genetic algorithm was provided by Yukun Hu et al. (2017). A set of fuzzy criteria that were flexible enough to accommodate various trade-offs between the bloom target discharge temperature, temperature uniformity, and particular fuel consumption enabled them to implement the zone model straight into a population-based genetic algorithm. The results indicated that the proposed furnace model provided insight into the dynamic heating behaviour with regard to the multi-objective criteria after multiple cases involving these trade-offs were tested [45].

In addition, Yukun Hu et al. (2018) used a zone method-based model with a self-adapting predictive control scheme to demonstrate a nonlinear dynamic simulation of actual transient furnace operation. It was discovered that the suggested model could dynamically adapt to variations in furnace operation with deviations of roughly 10°C from the measured discharge temperature. With regard to stability and fuel consumption (a 6% fuel savings compared to the previous scheme), the self-adapting predictive control strategy for furnace control was found to be superior [46].

To optimise and estimate the temperature of the billets inside the pusher type reheating furnace, G. Astolfi et al. (2017) proposed an Advanced Process Control system based on a two-layer linear Model Predictive Control technique. For internal process dynamics, a second black-box technique has been used in order to generate a global modelization of the furnace unit. Ad hoc constrained optimisation problems were used to change the online thermodynamic parameters that were needed for the nonlinear model formulation. An Italian patent for the suggested reheating furnace control technology has been granted [47].

In order to identify distribution of slab thermal efficiency (STE), Demin Chen et. al. (2018) presented a slab region thermal efficiency (SRTE) model and a STE model based on energy apportionment model of the reheating furnace and by considering

regional energy balance equation. Then, by performing partial correlation analysis on billet samples, which were obtained based on difference between the temperature of the billet when it was loaded and the time it spent in the reheating furnace, bottleneck of slab thermal efficiency (BSTE) was attained. A case study that used BSTE index values of 42% for preheating, 18% for heating II, 19% for soaking, 12% for heating I, and 9% for preheating and heating illustrated and verified these models. Preheating zone was therefore the primary area utilised to enhance STE [48].

A comprehensive data-driven framework for optimisation of combustion system operations was created by Zhenhao Tang et al. in 2019. An approach based on deep belief networks was created to model NOx emission as well as combustion efficiency. The deep belief network-based models were also combined to create a multi-objective optimisation model. The recently introduced swarm intelligence technique, the JAYA algorithm, was used to achieve the best solutions of proposed optimisation model because of nonlinearity and complexity of optimisation model. Results showed that by optimising the control settings of combustion system, it is possible to further improve both combustion efficiency and NO_x emission [49].

2. **Obtaining View-Factor Matrix Using Monte Carlo Method:** Thermal radiation calculations Energy and geometry are the two components that make up heat transfer between two surfaces. Heat exchange between surfaces in furnace enclosure, which is determined by view-factor matrix, is primary factor in the calculation of thermal radiation. The furnace presents a complicated geometry for view-factor computation since some of the surfaces in the enclosure cannot see each other and some can only be partially seen. Issues in thermal radiation are particularly well suited to this approach because energy moves in discrete photon bundles in a straight path before colliding with a surface. A high number of photons are emitted from the surface in case of determining view-factors in accordance with probability density functions. Each photon is tracked along its course, including any potential reflections, until it is absorbed at one of the furnace surfaces by treating photon emission and reflection as grey and diffuse.

The Monte Carlo approach requires emission and tracing the history of statistically significant random sample of photons from their places of emission to their absorption points, including numerous reflections, in order to determine view-factor matrix inside the furnace. The point and the direction of emission determine the emission of a single photon from a surface.

$$F_{i \to j} = \lim_{N_i \to \infty} \left(\frac{N_{i \to j}}{N_i} \right) \approx \left(\frac{N_{i \to j}}{N_i} \right)_{N_i >> 1} \qquad (27)$$

In order to improve the temperature of reheating furnace as well as quality of the slab heating, Waelen et al. devised an administrative control system to decide the furnace operating temperature. Researchers created the slab heating and two-dimensional heat conduction models, then used discretization to solve the mathematical model. They applied a mathematical solution in real time for a particular grade of steel using cheap computer resources. Therefore, there is good agreement between predicted and experimental outcomes [84]. The heat conduction equations for a slab are solved using

the boundary condition of radiative heat flux [50]. Calculations for the radiant energy are as follows:

$$Q_{Radiation} (n\theta) = \sigma A \left(\alpha_{slab} \, \varepsilon_{refractory} \, \frac{\sum(A_{h,i} T_{h,i}^4(n\theta))}{A_{h,i}} - \varepsilon_{slab} \, T_2^4(n\theta) \right) \quad (28)$$

Where, σ, α, ε are Stefan-Boltzmann constant, absorptivity and emissivity of grey body, hemispherical equivalent area is $A_{h,i}$ at corresponding temperature $T_{h,i}$.

Chen et. al. developed a technique for heating slabs in a reheating furnace optimally. The energy consumption of reheating furnace in the hot strip mill was managed using an arctangent function as the heating curve. They looked at whether heating thinner steel slabs in a reheating furnace uses less energy than heating thicker slabs. By using a heating curve with time and slab's dwell time in the reheat furnace, they were able to manage the temperature homogeneity of slab surface. Additionally, residence time and heating curve have an impact on energy usage and lower fuel consumption. In the furnace enclosure, radiation heat transfer is the predominant kind of heat transmission. Therefore, convective and conductive heat transport and radiation have a relatively small impact on the slab's surface temperature [51].

Heating curve: $T_s' = 0.5 + 0.475 Arc \, tan[1.75(2z' - 1)]$, where $T_s' = \frac{T_s - T_c}{T_d - T_c}$ and $z' = \frac{z}{L}$
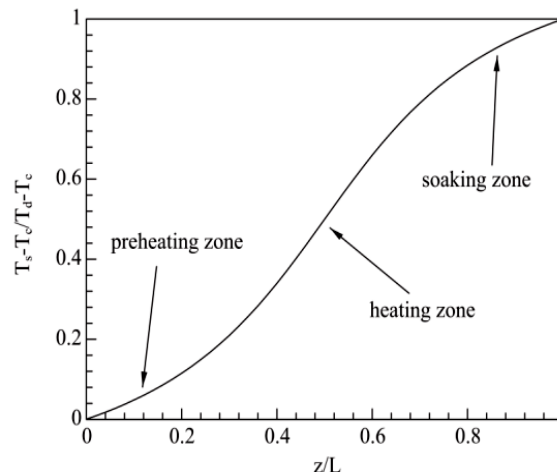
$$(29)$$

Figure 18: Representative Arctangent Curve for Slab Surface Temperature in Reheating Furnace[51]

The arctangent function can describe a typical heating curve on presumption that slab surface temperature is in equilibrium. Due to the structure of the arctangent heating curve, it was found that temperature differential between slab surface and centre increases quickly. After the heating period has passed through the inflection point, the interior temperature of the slab has a tendency to be uniform. This method has the advantage of simultaneously controlling the slab's goal temperature and a uniform temperature distribution inside the slab, which lowers energy usage [51].
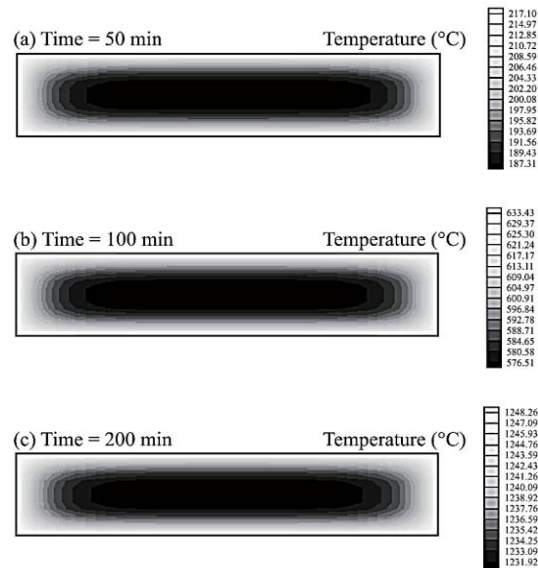
Figure 19: Isothermal Contours Inside Slab at Various Holding Time[51]

As can be observed from figure19, the most of heat transport from surface to the core occurs along the y-direction, resulting in very low isothermal lines differences. As a result, variations along the gauge length have a big impact on the temperature variation of slabs, while variations along the width direction have a much less impact [85].As can be observed from figure20, when the slab gauge is fixed at 250 mm, different widths have an impact on the transient distributions of maximum and minimum temperature difference. As a result, the temperature homogeneity of the slabs is not considerably impacted by width variation. However, the thickness of the slab has a big impact on how the temperature is distributed. The thickness of the slab causes a decrease in the temperature homogeneity of the slab [51].
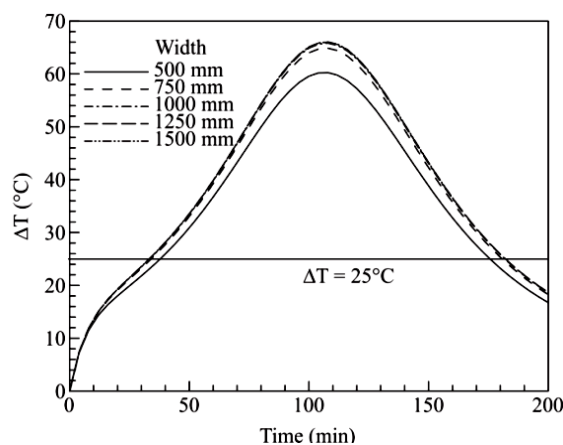
Figure 20: Effect of the Gauge Fixed at 250 Mm on Temperature Uniformity at Various Slab Widths [51]
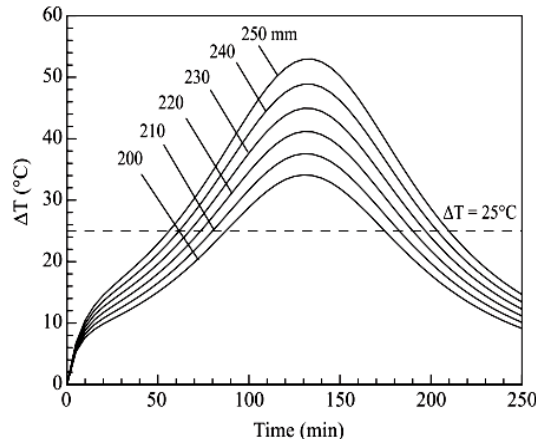
Figure 21: Effect of Slab Width Fixed at 1250 Mm on Temperature Uniformity at Various Slab Gauges[51]

On the basis of several variable parameters, including fuel consumption, fuel-to-airratio, fuel feeding rate, calorific value of the fuel, and total heat exchange factor along the length of reheating furnace, Miao et al. computed the productivity by examining the impact of heating profile of slabs. To determine the temperature history of furnace and slab, they determined the overall exchange factor. Due to its extremely low processing cost and straightforward approach, the total heat exchange factor method is widely employed in online control and mathematical models in reheating furnaces. They noticed that when the overall heat exchange factor, ϕ_{CF}, along the length of furnaces decreased, whereas, fuel consumption, fuel-to-air ratio, and calorific value of fuel all increased. The following relationship is used to compute the total heat exchange factor [52].

$$\phi_{CF} = \frac{q_{r,s_m} + q_{c,s_m}}{E_{b_t} - E_{b_{s_m}}} \qquad (30)$$

where, sum of the radiation and convection heat flux on the slab surface serves as the numerator, and difference between the black body radiation at slab's hot point and its surface serves as the denominator [52].

By implementing different size, energy analysis, and modification of the preheating zone, Kangvanskole et al. examined the technique to reduce the fuel energy consumption and improved efficiency of the reheating furnace. They concentrated on minimising sensible energy losses and preheating the slabs using flue gases in the preheating zone. The observed that the reheating chamber reduced the fuel energy consumption by 0.95%, 1.47%, 1.76%, and 1.87%, respectively, compared to the furnace without reheating chamber, as slab temperatures increased from the ambient temperature of 30°C to 59.53°C, 75.97°C, 84.97°C, and 89.45°C, respectively. Additionally, reheating furnace efficiency increased from 69.88% to 70.54%, 70.92%, 71.13%, and 71.22%, respectively [53]. To compute the temperature field of the stocks, Lindholm developed a 3D mathematical model based on finite element methods. It was discovered that model is in good conformation with analytical and numerical solution as well as the complete scale of experimental data. The effect of radiation shadowing on skid pipes, uneven slab heating, the impact of baffles in the furnace, and end effects in the stocks were all

anticipated by the 3D finite element code [54]. Ju et al. proposed a mathematical model for the steady state condition of a pusher type reheat furnace based on the three zone method. They discovered that, when the subzone's size is larger, the experimental results after validation do not support the projected results [55]. To lower production costs and improve energy efficiency in walking hearth type reheating furnaces, Srisertpol et al. suggested a mathematical solution. By adopting less expensive fuels like natural gas, biogas, etc., they improved the efficiency of temperature control reheating furnaces and reduced energy usage. In order to construct the controller, they used a mathematical model that combined a non-linear least squares pattern search algorithm with open-loop identification [56]. Researchers are currently working to lower production costs and improve reheating furnace performance.

V. CONCLUSION

Following an extensive review of the existing literature, multiple approaches are being employed to optimise the duration of slab residence within the reheating furnace and enhance its efficiency. These methods include numerical modelling utilising proprietary software, CFD modelling employing commercially available codes, and the utilisation of other correlating mathematical models. CFD modelling, when combined with an in-house User-Defined Function (UDF) code, has the potential to yield exceptionally accurate outcomes. Consequently, this approach emerges as a cost-effective and time-efficient alternative to online simulation approaches. Additional investigation can be conducted via computational fluid dynamics (CFD) modelling in order to mitigate the computational burden. Furthermore, fresh approaches can be devised to enhance the duration of slab occupancy within reheating furnaces while concurrently improving their efficiency.

REFERENCES

[1] S.G. Jansto, Reheat furnace operational parameters affecting hot roll quality of microalloyed long products, (2015).
[2] D.R. Kreuzer, A. Werner, D.R.K.A. Werner, Implementation of Models for reheating processes in industrial furnaces, (2011) 376–387. https://doi.org/10.3384/ecp11063376.
[3] W. Trinks, Industrial furnaces, J. Franklin Inst. 254 (1952) 186. https://doi.org/10.1016/0016-0032(52)90645-5.
[4] P.K. Thakur, S.K. Prakash, K.G. Murlidharan, S.S. Das, A review on efficient energy optimization in reheating furnaces, (2014) 43–49.
[5] P. Marino, a. Pignotti, D. Solis, Control of pusher furnaces for steel slab reheating using a numerical model, Lat. Am. Appl. Res. 34 (2004) 249–255.
[6] T. Morgado, P.J. Coelho, P. Talukdar, Assessment of uniform temperature assumption in zoning on the numerical simulation of a walking beam reheating furnace, Appl. Therm. Eng. 76 (2015) 496–508. https://doi.org/10.1016/j.applthermaleng.2014.11.054.
[7] P. Kumar, Training Manual on Energy Efficiency for Small and Medium Enterprises, 2010. http://www.apo-tokyo.org/00e-books/GP-21_TMEE/GP-21_TMEE.pdf.
[8] M. Zajemska, A. Poskart, M. Zajemska, A. Poskart, Modellazione Prediction of the chemical composition of combustion products in metallurgical reheating furnaces by use of numerical methods Memorie, (n.d.) 33–40.
[9] S. Dutte, A. Gupta, Hearth and skid pipe refractories for reheating furnace - A Review, (n.d.) 94–102.
[10] C. Zhang, T. Ishii, S. Sugiyama, Numerical Modeling of the Thermal Performance of Regenerative Slab Reheat Furnaces, Numer. Heat Transf. Part A Appl. 32 (1997) 613–631. https://doi.org/10.1080/10407789708913909.
[11] Jong Gyu Kim, Kang Y. Huh, Il Tae K, Three-Dimensional Analysis of the Walking-Beam-Type Slab Reheating Furnace in Hot Strip Mills, Numer. Heat Transf. Part A Appl. 38 (2000) 589–609.

https://doi.org/10.1080/104077800750021152.

[12] Y. Tang, J. Laine, T. Fabritius, J. Härkki, The Modeling of the Gas Flow and Its Influence on the Scale Accumulation in the Steel Slab Pusher-type Reheating Furnace, ISIJ Int. 43 (2003) 1333–1341. https://doi.org/10.2355/isijinternational.43.1333.

[13] C.-T. Hsieh, M.-J. Huang, S.-T. Lee, C.-H. Wang, A Numerical Study of Skid Marks on the Slabs in a Walking-Beam Type Slab Reheating Furnace, Numer. Heat Transf. Part A Appl. 57 (2010) 1–17. https://doi.org/10.1080/10407780903529308.

[14] C.-T. Hsieh, M.-J. Huang, S.-T. Lee, C.-H. Wang, Numerical Modeling of a Walking-Beam-Type Slab Reheating Furnace, Numer. Heat Transf. Part A Appl. 53 (2008) 966–981. https://doi.org/10.1080/10407780701789831.

[15] S.H. Han, D. Chang, C.Y. Kim, A numerical analysis of slab heating characteristics in a walking beam type reheating furnace, Int. J. Heat Mass Transf. 53 (2010) 3855–3861. https://doi.org/10.1016/j.ijheatmasstransfer.2010.05.002.

[16] S.H. Han, D. Chang, Optimum residence time analysis for a walking beam type reheating furnace, Int. J. Heat Mass Transf. 55 (2012) 4079–4087. https://doi.org/10.1016/j.ijheatmasstransfer.2012.03.049.

[17] M. Gu, G. Chen, X. Liu, C. Wu, H. Chu, Numerical simulation of slab heating process in a regenerative walking beam reheating furnace, Int. J. Heat Mass Transf. 76 (2014) 405–410. https://doi.org/10.1016/j.ijheatmasstransfer.2014.04.061.

[18] V.K. Singh, P. Talukdar, P.J. Coelho, Performance Evaluation of Two Heat Transfer Models of a Walking Beam Type Reheat Furnace, Heat Transf. Eng. 36 (2015) 91–101. https://doi.org/10.1080/01457632.2014.906287.

[19] J.M. Casal, J. Porteiro, J.L. Míguez, A. Vázquez, New methodology for CFD three-dimensional simulation of a walking beam type reheating furnace in steady state, Appl. Therm. Eng. 86 (2015). https://doi.org/10.1016/j.applthermaleng.2015.04.020.

[20] ANSYS, ANSYS FLUENT 12.0 UDF Manual, in: ANSYS Fluent User's Man., 2009: pp. 724–746.

[21] ANSYS, Fluent - User's guide, in: ANSYS Fluent User's Man., 1992: p. 727. https://doi.org/10.1016/0167-4048(92)90125-B.

[22] T.-H. Shih, W.W. Liou, A. Shabbir, Z. Yang, J. Zhu, A new k-ε eddy viscosity model for high reynolds number turbulent flows, Comput. Fluids. 24 (1995) 227–238. https://doi.org/10.1016/0045-7930(94)00032-T.

[23] R.W. Bilger, Turbulent Jet Diffusion Flames, Prog. Energy Combust. Sci. 1 (2006) 87–109.

[24] P.A. Libby, F.A. Williams, Turbulent reacting flows, Academic Press, London; New York, 1994.

[25] W.P. Jones, J.H. Whitelaw, Calculation methods for reacting turbulent flows: A review, Combust. Flame. 48 (1982) 1–26. https://doi.org/10.1016/0010-2180(82)90112-2.

[26] M.F. Modest, The Weighted-Sum-of-Gray-Gases Model for Arbitrary Solution Methods in Radiative Transfer, J. Heat Transfer. 113 (1991) 650. https://doi.org/10.1115/1.2910614.

[27] Y. Yang, J. Kroeze, M. a. Reuter, Simulation of slab movement and transient heating in a continuous steel reheat furnace, Prog. Comput. Fluid Dyn. An Int. J. 4 (2004) 46. https://doi.org/10.1504/PCFD.2004.003785.

[28] M.J. Huang, C.T. Hsieh, S.T. Lee, C.H. Wang, A coupled numerical study of slab temperature and gas temperature in the walking-beam-type slab reheating furnace, Numer. Heat Transf. Part A Appl. 54 (2008) 625–646. https://doi.org/10.1080/10407780802289475.

[29] M. Venturino, P. Rubini, Coupled fluid flow and heat transfer analysis of steel reheat furnaces, 3rd Eur. Conf. Ind. Furn. Boil. (1995) 8.

[30] Y. Hu, C.K. Tan, J. Broughton, E. McGee, A. Matthew, P.A. Roach, Development of Transient Mathematical Models for a Large-scale Reheating Furnace Using Hybrid Zone-CFD Methods, Energy Procedia. 75 (2015) 3076–3082. https://doi.org/10.1016/j.egypro.2015.07.633.

[31] J. Zhang, L.I.U. Qing, S. Yang, Z. Chen, L.I. Jingshe, Z. Jiang, Advances in Ladle shroud as a functional device in tundish metallurgy: A review, ISIJ Int. 59 (2019) 1167–1177. https://doi.org/10.2355/isijinternational.ISIJINT-2019-044.

[32] S. Chakraborty, A. Rajora, S.P. Singh, P. Talukdar, Heat transfer and discrete phase modelling of coal combustion in a pusher type reheating furnace, Appl. Therm. Eng. 116 (2017) 66–78. https://doi.org/10.1016/j.applthermaleng.2017.01.056.

[33] G. Tang, B. Wu, D. Bai, Y. Wang, R. Bodnar, C.Q. Zhou, Modeling of the slab heating process in a walking beam reheating furnace for process optimization, Int. J. Heat Mass Transf. 113 (2017) 1142–1151. https://doi.org/10.1016/j.ijheatmasstransfer.2017.06.026.

[34] Z. Ahmed, S. Lecompte, T. De Raad, M. De Paepe, Steady State model of a Reheating Furnace for

determining slab boundary conditions, Energy Procedia. 158 (2019) 5844–5849. https://doi.org/10.1016/j.egypro.2019.01.542.

[35] Y. Liu, J. Wang, C. Min, G. Xie, B. Sundén, Performance of fuel-air combustion in a reheating furnace at different flowrate and inlet conditions, Energy. 206 (2020). https://doi.org/10.1016/j.energy.2020.118206.

[36] Y. Tang, J. Laine, T. Fabritus, J. Härkk, Different methods obtained by PHOENICS simulation to improve the performance of pusher-type steel slab reheating furnace, 2002.

[37] Y. Yang, Y. Lu, Development of a computer control model for slab reheating furnaces, Comput. Ind. 7 (1986) 145–154. https://doi.org/10.1016/0166-3615(86)90036-9.

[38] Y. Yang, Y. Lu, Dynamic model based optimization control for reheating furnaces, Comput. Ind. 10 (1988) 11–20. https://doi.org/10.1016/0166-3615(88)90044-9.

[39] W.H. Chen, Y.C. Chung, J.L. Liu, Analysis on energy consumption and performance of reheating furnaces in a hot strip mill, Int. Commun. Heat Mass Transf. 32 (2005) 695–706. https://doi.org/10.1016/j.icheatmasstransfer.2004.10.019.

[40] A. Jaklič, T. Kolenko, B. Zupančič, The influence of the space between the billets on the productivity of a continuous walking-beam furnace, Appl. Therm. Eng. 25 (2005) 783–795. https://doi.org/10.1016/j.applthermaleng.2004.07.012.

[41] A. Jaklič, F. Vode, T. Kolenko, Online simulation model of the slab-reheating process in a pusher-type furnace, Appl. Therm. Eng. 27 (2007) 1105–1114. https://doi.org/10.1016/j.applthermaleng.2006.07.033.

[42] S.H. Han, S.W. Baek, S.H. Kang, C.Y. Kim, Numerical analysis of heating characteristics of a slab in a bench scale reheating furnace, Int. J. Heat Mass Transf. 50 (2007) 2019–2023. https://doi.org/10.1016/j.ijheatmasstransfer.2006.10.048.

[43] M. Safari, A. Saboonchi, Simulation of temperature distribution in a continuous tunnel reheat furnace using monte carlo method, Int. J. ISSI. 5 (2008) 1–7.

[44] W. Zhou, T. Qiu, Zone modeling of radiative heat transfer in industrial furnaces using adjusted Monte-Carlo integral method for direct exchange area calculation, Appl. Therm. Eng. 81 (2015) 161–167. https://doi.org/10.1016/j.applthermaleng.2015.02.004.

[45] Y. Hu, C.K. Tan, J. Broughton, P.A. Roach, L. Varga, Model-based multi-objective optimisation of reheating furnace operations using genetic algorithm, Energy Procedia. 142 (2017) 2143–2151. https://doi.org/10.1016/j.egypro.2017.12.619.

[46] Y. Hu, C.K. Tan, J. Broughton, P.A. Roach, L. Varga, Nonlinear dynamic simulation and control of large-scale reheating furnace operations using a zone method based model, Appl. Therm. Eng. 135 (2018) 41–53. https://doi.org/10.1016/j.applthermaleng.2018.02.022.

[47] G. Astolfi, L. Barboni, F. Cocchioni, C. Pepe, S.M. Zanoli, Optimization of a pusher type reheating furnace: An adaptive Model Predictive Control approach, 2017 6th Int. Symp. Adv. Control Ind. Process. AdCONIP 2017. (2017) 19–24. https://doi.org/10.1109/ADCONIP.2017.7983749.

[48] D. Chen, B. Lu, F.Q. Dai, G. Chen, X. Zhang, Bottleneck of slab thermal efficiency in reheating furnace based on energy apportionment model, Energy. 150 (2018) 1058–1069. https://doi.org/10.1016/j.energy.2018.02.149.

[49] Z. Tang, Z. Zhang, The multi-objective optimization of combustion system operations based on deep data-driven models, Energy. 182 (2019) 37–47. https://doi.org/10.1016/j.energy.2019.06.051.

[50] a. a. Waelen, B. Young, W. Yu, Adaptive Supervisory Control of an Industrial Steel Slab Reheating Furnace, Chem. Prod. Process Model. 4 (2009). https://doi.org/10.2202/1934-2659.1449.

[51] W. Chen, M. Lin, T. Leu, Optimal heating and energy management for slabs in a reheating furnace, 18 (2010) 24–31.

[52] M. Cuim, H.G. Chen, L. Xu, B. Wu, Total Heat Exchange Factor Based on Non-Gray Radiation Properties of Gas in Reheating Furnace, J. Iron Steel Res. Int. 16 (2009) 27–31. https://doi.org/10.1016/S1006-706X(09)60039-X.

[53] K. Kangvanskol, C. Tangthieng, An Energy Analysis of a Slab Preheating Chamber for a Reheating Furnace, Eng. J. 18 (2014) 1–12. https://doi.org/10.4186/ej.2014.18.2.1.

[54] D. Lindholm, B. Leden, A finite element method for solution of the three-dimensional time-dependent heat-conduction equation with application for heating of steels in reheating furnaces, Numer. Heat Transf. Part A Appl. 35 (1999) 155–172. https://doi.org/10.1080/104077899275308.

[55] Y. Ju, J. Hsieh, Numerical analysis of heat transfer in a slab reheating furnace, J. Chinese Inst. Eng. 13 (1990) 341–346. https://doi.org/10.1080/02533839.1990.9677262.

[56] J. Srisertpol, S. Tantrairatn, P. Tragrunwong, V. Khomphis, Temperature control for reheating furnace walking hearth type in heating curve up process, in: Int. Conf. Syst. Sci. Simul. Eng. - Proc., 2010: pp. 464–469.